Non-linear thermal gradients shape broad-scale patterns in geographic range size and can reverse Rapoport's Rule: Appendix A

Authors: Adam Tomašových, David Jablonski, Sarah K. Berke, Andrew Z. Krug, James W. Valentine

Supplementary text, references, figures and tables

Data sets and spatial scale of analyses

Species occurrences were compiled from the literature and museum collections, causing variable spatial resolution of individual occurrences among different regions (median. occurrence resolution = 1.2°). Range interpolation (i.e., adding species to all cells that are situated within latitudinal range limits) did not change the outcomes of analyses of gradients in range size, and we therefore used raw distributions. Data were downloaded from the bivalve database (Jablonski et al. 2013) on 19 March 2014. The datasets are available from Data Dryad at dx.doi.org/10.5061/dryad.6n15h.

Definitions of oceanic margins

Localities with occurrence data used in this study are derived from the three best-sampled oceanic margins (or latitudinal "transects") -- the Western Pacific (gray squares), Eastern Pacific (black diamonds), and Western Atlantic (gray triangles). We separate western from eastern oceanic margins because they are characterized by qualitatively different latitudinal gradients in sea-surface temperature (SST) (Fig. A1). The Earth's rotation drives warm tropical waters toward the poles along the western margins of ocean basins and polar water toward the equator along the eastern margins. Therefore, tropical zones with SSTs of 26-27°C are about 3,000-3,500 km in N-S breadth along the western margins but only about 1,500 km in breadth along the Eastern Pacific. The tropical belt is thus broader and latitudinal gradients in annual SST minima, means, and maxima are markedly non-linear within each hemisphere along the western margins. The Eastern Pacific transect starts at the Beaufort Sea, continues through the Aleutian Islands, along the Eastern Pacific shelf including offshore islands such as the Galapagos to the southern tip of South America. The Western Pacific transect starts in the western part of the Chukchi Sea, proceeds south along the Asian continental margin, but also includes the Okhotsk Sea, the Sea of Japan, Taiwan, the Philippines, Indonesia, New Guinea and the east coast of Australia and New Zealand, ending in Antarctica; we incorporate the occurrences on the major islands in this transect because they constitute part of a single West Pacific realm (Valentine 1973, Spalding et al. 2007), and we are interested in tracing maximum diversity and greatest sampling density. The Western Atlantic transect starts in the Greenland Sea, includes Ellesmere Island and Baffin Island, proceeds south along the eastern America margin to the southern tip of South America and the eastern part of the Antarctic Peninsula (Fig. A2). The West African fauna remains too poorly resolved for a comparable analysis in the Eastern Atlantic. The Eastern Pacific with 1043 species shares 149 species with the Western Pacific (3134 species) and 164 species with the Western Atlantic (946 species), almost entirely along its high northern margins. The Western Atlantic shares 123 species with the Western Pacific, almost entirely along its high-latitude northern and southern margins.

Thermal range size and temperature data

When measuring species thermal range, we use IQR because it is less sensitive than total range to the number of species occurrences, and thus tends to be less dependent on geographic range size. SSTs measured in 2009 were obtained at a 9 km spatial resolution from the Moderate Resolution Imaging Spectroradiometer (MODIS) carried by the Aqua satellite. MODIS data were derived from the 11 um channel with the highest quality flag and taken at daily resolution (podaac-opendap.jpl.nasa.gov/opendap/allData/modis/L3/aqua/ 11um/9km/daily). Similar results were obtained from the HadISST 1.1 database (UK Meteorological Office, Hadley Centre). Temperatures at 0 m, 50 and 100 m were obtained from the World Ocean Atlas 2005 at 1° latitude/longitude resolution. The macroecological thermal ranges of species measured at 50 and 100 meters isobaths significantly correlate with their thermal ranges as estimated from SSTs (Fig. A5), and latitudinal gradients in annual mean temperature at 50 m and 100 m have shapes similar to those at 0 m, while thermal differences between 0 and 100 m at similar latitudes are much smaller than differences in SST between low-latitude and mid-latitude habitats (Fig. A5).

The per-band latitudinal range size is measured as the median of all ranges that occur in that band (this is similar to Stevens' method based on means). The midpoint method that counts only ranges whose midpoint falls in a given band (Rohde et al. 1993) is not appropriate here because Rapoport's rule relates to all species that intersect a given region, not just to species with their range midpoint in a given region. When measuring the clustering of range limits along latitudinal gradients, we removed the highest-latitude band from each hemisphere because 100% of species in those bands have range limits there.

Range-shuffling null model

This model incorporates (1) the relationship between per-band range size and latitude expected from the reduction of latitudinal range size of ranges overlapping the poles (Colwell and Hurtt 1994), (2) longitudinal sampling variability that can generate spurious gradients in range size (narrow-ranging species will be more likely sampled in better sampled latitudes), and (3) the non-independence of range-size estimates in each band, because the same species can contribute to multiple bands and species range sizes may be spatially autocorrelated. The source code is available at http://datadryad.org/handle/10255/dryad.68917.

Range midpoints are determined by randomly drawing coordinates of shelf cells separately within each oceanic margin, weighting the selection probability of each 1° cell at a given latitude by its longitudinal diameter (we exclude all continental and oceanic cells), accounting for the fact that the total area of latitudinal bands decreases with latitude. Empirical latitudinal and longitudinal ranges are then used to generate rectangles around these midpoints. If northern or southern range limits are not located on the shelf, the random sampling of midpoints is repeated and the range midpoint is re-positioned, thus approximately conserving the transect-level empirical distribution of latitudinal range sizes. We thus follow the range rejection algorithm in Sandel and McKone 2006 (see also McClain et al. 2007). To account for the edge effects, the portions of ranges that would be placed outside the grid edge are transported into the adjacent hemisphere so that geographic ranges are not artificially truncated by grid edges. For example, if the range midpoint is placed at 80°S and at 90°E and its latitudinal radius is ~2000 km, thus approximately 20° to the north and south (and crossing the Northern Pole), one equatorward range limit will be at 60°S and 90°E and another equatorward range limit will be at 80°S and 90°W. Finally, species are sampled in those 1° cells that are present in the empirical database, and the latitudinal and macroecological thermal ranges are computed for each species. We repeat this procedure in 1000 runs for each transect, drawing range sizes only from the species pool of a given transect

Predictions for temperature-limited models

In the body of this paper we report on model results for the median temperature-limited scenario, with assumptions and output that lie between the scenarios we term "stringent" and "relaxed" (Fig. A8). Although model predictions can differ because latitudinal gradients in temperature minima and maxima derived from the MODIS and HadISST 1.1 databases differ slightly, estimates of SST minima and maxima at each latitude can differ if they are averaged across all longitudes or just across longitudes that correspond to shelf depths, and per-band estimates of range sizes differ depending on the width of latitudinal bands (computed per 1°, 5° or 10°), these sources of variation generate differences in predictions that are smaller than differences in predictions between the three major scenarios. All three scenarios predict that range size is expected to increase towards the tropics along the western oceanic margins.

In the relaxed temperature-limited scenario, species expand to latitudes where the minimum and maximum temperatures fall within the temperature bounds at its latitude of origination for at least one month. For example, polar ectotherms can shut down their metabolism during most of the year and feed during a few months when summer conditions allow primary productivity, essentially hibernating during the rest of the year (Brockington et al. 2001). We find that: (a) latitudinal ranges in the Western Pacific and Western Atlantic attain 8,000 km because species that were initially placed ("originated") at mid latitudes can expand their ranges farther into the opposite hemisphere (Fig. A9), (b) thermal ranges at low latitudes are still narrower in the tropics than at mid latitudes along the western margins (although the differences among latitudes are smaller than in the median temperature-limited scenario), and thermal ranges are relatively uniform in size in the Eastern Pacific, and (c) low latitudes contain few range limits per latitudinal bin at low latitudes and are bounded by sharp peaks in the proportions of poleward limits at latitudes where mean annual temperature changes more steeply, as seen in the median temperature-limited scenario.

In the median temperature-limited scenario, two subtle and narrow peaks corresponding to ranges reaching 6,000 km occur near 30° S and N in the Western Pacific and Western Atlantic, corresponding to latitudes where maximum temperature exceeds the mean sea-surface temperature at the equator, allowing some species that were initially placed in environments with a broad annual temperature range to expand their ranges across the entire tropics. In the relaxed temperature-limited scenario, even more species that were initially placed in environments with a broad annual temperature range are thus allowed to expand their ranges across the entire tropics, thus strongly increasing range sizes at low latitudes.

In the stringent temperature-limited scenario, (a) median latitudinal range is also largest at low latitudes but only attains 2,000-4,000 km (Fig. A10). (b) Thermal ranges attain (small) maxima at low latitudes because latitudinal ranges are extremely limited at higher latitudes, and (c) the clustering of range limits is very strong along the entire gradient, although some minima still occur at low latitudes. The source code is available at http://datadryad.org/handle/10255/dryad.68987.

Supplemental references - additional citations by topic:

1. Empirical analyses of range-size gradients and tests of Rapoport's rule (Rohde et al. 1993; Rohde and Heap 1996; Stevens 1996; Rohde 1999; Harcourt 2000; Diniz-Filho and Tôrres 2002; Hughes et al. 2002; Macpherson 2003; Mora et al. 2003; Smith and Gaines 2003; Fortes and R. S. Absalao 2004; Bellwood et al. 2005; Cruz et al. 2005; Hausdorf 2006; Rangel et al. 2006; Stauffer and Rohde 2006)
2. Effects of temperature on range limits and species distributions (Gaylord and Gaines 2000; Brockington et al. 2001; Clarke 2003; Gilman 2006; Compton et al. 2007; Lima et al. 2007; Gutierrez et al. 2008; Beukema et al. 2009; Herbert et al. 2009)
3. Null models predicting range-size gradients (Colwell and Hurtt 1994; Colwell and Lees 2000; Romdal et al. 2005; Sandel and McKone 2005; Ribas and Schoereder 2006; Colwell et al. 2009)

References

Bellwood, D.R., Hughes, T.P., Connolly, S.R. & Tanner, J. (2005) Environmental and geometric constraints on Indo-Pacific coral reef biodiversity. *Ecology Letters,* **8**, 643-651.

Beukema J.J, Dekker R. & Jansen, J.M. (2009) Some like it cold: populations of the tellinid bivalve *Macoma balthica* (L.) suffer in various ways from a warming climate. *Marine Ecology-Progress Series*, **384**, 135-145.

Brockington, S., Clarke, A. & Chapman, A.L.G. (2001) Seasonality of feeding and nutritional status during the austral winter in the Antarctic sea urchin *Sterechinus neumayeri*. *Marine Biology*, **139**, 127–138

Clarke, A. (2003) Costs and consequences of evolutionary temperature adaptation. *Trends in Ecology and Evolution*, **18**, 573-581.

Colwell, R.K. & Hurtt, G.C. (1994) Nonbiological gradients in species richness and a spurious Rapoport effect. *American Naturalist*, **144**, 570-595.

Colwell, R.K. & Lees, D. 2000. The mid-domain effect: geometric constraints on the geography of species richness. *Trends in Ecology and Evolution* 15:70-76.

Colwell, R.K, Gotelli, N.J., Rahbek, C., Entsminger, G.L., Farrell, C. & Graves,G.R. (2009) Peaks, plateaus, canyons, and craters: the complex geometry of simple mid-domain effect models. *Evolutionary Ecology Research,* **11**, 355-370.

Compton, T.J., Rijkenberg, M.J.A., Drent, J. & Piersma, T. (2007) Thermal tolerance ranges and climate variability: A comparison between bivalves from differing climates. *Journal of Experimental Marine Biology and Ecology*, **352**, 200-211.

Cruz, F.B., Fitzgerald, L.A., Espinoza, R.E. & Schulte, J.A. (2005) The importance of phylogenetic scale in tests of Bergmann's and Rapoport's rules: lessons from a clade of South American lizards. *Journal of Evolutionary Biology*, **18**, 1559–1574.

Diniz-Filho, J.A. F. & Tôrres, N.M. (2002) Rapoport effect in South American Carnivora (Mammalia): null models under geometric and phylogenetic constraints. *Brazilian Journal of Biology*, **62**, 437–444.

Fortes, R.R. & Absalao, R.S. (2004) The applicability of Rapoport's Rule to the marine molluscs of the Americas. *Journal of Biogeography*, **31**, 1909-1916.

Gaylord, B. & Gaines, S.D. (2000) Temperature or transport? Range limits in marine species mediated solely by flow. *American Naturalist*, **155**, 769–789.

Gilman, S.E. (2006) The northern geographic range limit of the intertidal limpet *Collisella scabra*: a test of performance, recruitment, and temperature hypotheses. *Ecography*, **29**, 709–720.

Gutierrez, N.L., Martinez, A. & Defeo, O. (2008) Identifying environmental constraints at the edge of a species' range: scallop *Psychrochlamys patagonica* in the SW Atlantic Ocean. *Marine Ecology-Progress Series,* **353**, 147-156.

Harcourt, A.H. 2000. Latitude and latitudinal extent: a global analysis of the Rapoport effect in a tropical mammalian taxon: primates. *Journal of Biogeography*, **27**, 1169-1182.

Hausdorf, B. 2006. Latitudinal and altitudinal diversity patterns and Rapoport effects in north-west European land snails and their causes. *Biological Journal of the Linnean Society*, **87**, 309-323

Herbert, R.J.H., Southward, A.J., Clarke, R.T., Sheader, M. & Hawkins, S.J. 2009. Persistent border: an analysis of the geographic boundary of an intertidal species. *Marine Ecology-Progress Series,* **379**, 135-150.

Hughes, T.P., Bellwood, D.R. & Connolly, S.R. 2002. Biodiversity hotspots, centres of endemicity, and the conservation of coral reefs. *Ecology Letters*, **5**, 775-784.

Jablonski, D., Belanger, C.L., Berke, S.K., Huang, S., Krug, A.Z., Roy, K., Tomasovych, A. & Valentine, J.W. (2013) Out of the Tropics, but how? Fossils, bridge species, and thermal ranges in the dynamics of the marine latitudinal diversity gradient. *Proceedings of the National Academy of Sciences USA,* **110**, 10487-10494

Lima, F.P., Ribeiro, P.A., Queiroz, N., Xavier, R., Tarroso, P., Hawkins, S.J. & Santos, A.M. (2007) Modelling past and present geographical distribution of the marine gastropod Patella rustica as a tool for exploring responses to environmental change. *Global Change Biology,* **13**, 2065-2077

Macpherson, E. (2003) Species range size distributions for some marine taxa in the Atlantic Ocean. Effect of latitude and depth. *Biological Journal of the Linnean Society*, **80**, 437-455.

Mora, C., Chittaro, P. M., Sale, P., Kritzer, J.P. & Ludsin, S.A. (2003) Patterns and processes in reef fish diversity. *Nature*, **421**, 933-936.

Rangel, T.F.L.V.B., Diniz-Filho, A.F. & Bini, L.M. (2006) Towards an integrated computational tool for spatial analysis in macroecology and biogeography. *Global Ecology and Biogeography*, **15**, 321-327.

Ribas, C.R. & Schoereder, J.H. (2006) Is the Rapoport effect widespread? Null models revisited. *Global Ecology and Biogeography,* **15**, 614-624.

Rohde, K., Heap, M. & Heap, D. (1993) Rapoport's rule does not apply to marine teleosts and cannot explain latitudinal gradients in species richness. *American Naturalist*, **142**, 1-16.

Rohde, K. & Heap, M. (1996) Latitudinal ranges of teleost fish in the Atlantic and Indo-Pacific oceans. *American Naturalist*, **147**, 659–665.

Rohde, K. (1999) Latitudinal gradients in species diversity and Rapoport's rule revisited: a review of recent work and what can parasites teach us about the causes of the gradients? *Ecography*, **22**, 593-613.

Romdal, T.S., Colwell, R.K. & Rahbek, C. (2005) The influence of band sum area, domain extent, and range sizes on the latitudinal mid-domain effect. *Ecology*, **86**, 235–244.

Sandel, B.S. & McKone, M.J. (2006) Reconsidering null models of diversity: do geometric constraints on species ranges necessarily cause a mid-domain effect? *Diversity and Distributions*, **12**, 467-474.

Smith, K.F., & Gaines, S.D. 2003. Rapoport's bathymetric rule and the latitudinal species diversity gradient for Northeast Pacific fishes and Northwest Atlantic gastropods: evidence against a causal link. *Journal of Biogeography*, **30**, 1153-1159.

Stauffer, D. & Rohde, K (2006) Simulation of Rapoport's Rule for latitudinal species spread. *Theory in Biosciences*, **125**, 55-65.

Stevens, G.C. (1996) Extending Rapoport's rule to Pacific marine fishes. *Journal of Biogeography*, **23**, 149-154.

Table S1 AIC values for three different types of spatial correlation structure used in the generalized least-square models that evaluate the relation between empirical median latitudinal range size and latitude, and the relation between the empirical clustering of range limits and the steepness of temperature gradient.

	AIC-Exponential structure	AIC-Gaussian structure	AIC-Spherical structure
SW Pacific-range size-latitude relation	21.98	44.58	20.61
NW Pacific-range size-latitude relation	2.09	9.11	2.36
SE Pacific-range size-latitude relation	22.24	40.38	21.13
NE Pacific-range size-latitude relation	-34.14	-23.55	-33.48
SE Atlantic-range size-latitude relation	-0.05	26.70	-1.32
NW Atlantic-range size-latitude relation	-16.89	-13.34	-17.45
WP-poleward limits-temperature steepness relation	93.88	102.49	92.70
EP-poleward limits-temperature steepness relation	94.72	102.40	96.07
WA-poleward limits-temperature steepness relation	94.94	103.77	96.01

Table S2 Empirical data versus predictions of the null model and the median temperature-limited model: the generalized least-square slope of the relationship between log-transformed per-band median latitudinal range size and latitude is significantly more negative than predicted by the null model in the western transects, and is qualitatively similar to the predictions of the temperature-limited models. The p-value of the null model was computed as the proportion of 1000 simulations for which the value of the null slope equaled or was smaller than the empirical slope. WP – Western Pacific, WA – Western Atlantic, EP – Eastern Pacific.

Margin	Data-model	GLS slope	Lower 95% c.i.	Upper 95% c.i.	p-value (slope=0)
SW Pacific	Empirical data	-0.0417	-0.051	-0.0325	<0.001
NW Pacific	Empirical data	-0.0058	-0.0135	0.0018	0.125
SE Pacific	Empirical data	-0.0309	-0.0441	-0.0177	<0.001
NE Pacific	Empirical data	-0.0033	-0.0045	-0.0022	<0.001
SW Atlantic	Empirical data	-0.0148	-0.0236	-0.006	0.0029
NW Atlantic	Empirical data	-0.0026	-0.0062	0.0011	0.1521
SW Pacific	SST-limited model	-0.0189	-0.0393	0.0015	0.0659
NW Pacific	SST-limited model	-0.0053	-0.01	-6.00E-04	0.0305
SE Pacific	SST-limited model	-0.0184	-0.0273	-0.0095	<0.001
NE Pacific	SST-limited model	-0.0029	-0.0049	-8.00E-04	0.0109
SW Atlantic	SST-limited model	-0.0246	-0.0324	-0.0167	<0.001
NW Atlantic	SST-limited model	-0.006	-0.0091	-0.003	<0.001
SW Pacific	Null model	0.009868	0.0088614	0.0108111	<0.001
NW Pacific	Null model	0.0022956	0.0010928	0.0037572	<0.001
SE Pacific	Null model	0.0026252	0.0015894	0.0041715	<0.001
NE Pacific	Null model	-0.001456	-0.002318	-0.000341	<0.001
SW Atlantic	Null model	-0.006856	-0.008789	-0.004714	<0.001
NW Atlantic	Null model	-0.00368	-0.00559	-0.001869	<0.001

Table S3 Empirical data versus predictions of the null model and the median temperature-limited model: the generalized least-square slope of the relationship between the clustering (logit-transformed proportions) of poleward range limits and absolute spatial change in annual mean daily SST is significantly more positive than predicted by the null model and similar to the slope predicted by the temperature-limited model.

Margin	Data-model	GLS slope	Lower 95% c.i.	Upper 95% c.i.	p-value (slope=0)
Western Pacific	Empirical data	0.539	0.284	0.795	<0.001
Eastern Pacific	Empirical data	0.274	0.010	0.538	0.0427
Western Atlantic	Empirical data	0.439	0.284	0.594	<0.001
Western Pacific	SST-limited model	0.561	0.321	0.802	<0.001
Eastern Pacific	SST-limited model	0.407	0.138	0.582	<0.001
Western Atlantic	SST-limited model	0.663	0.420	0.906	<0.001
Western Pacific	Null model	- 0.046	-0.108	0.010	0.01
Eastern Pacific	Null model	0.053	-0.042	0.134	<0.001
Western Atlantic	Null model	- 0.096	-0.144	-0.045	<0.001

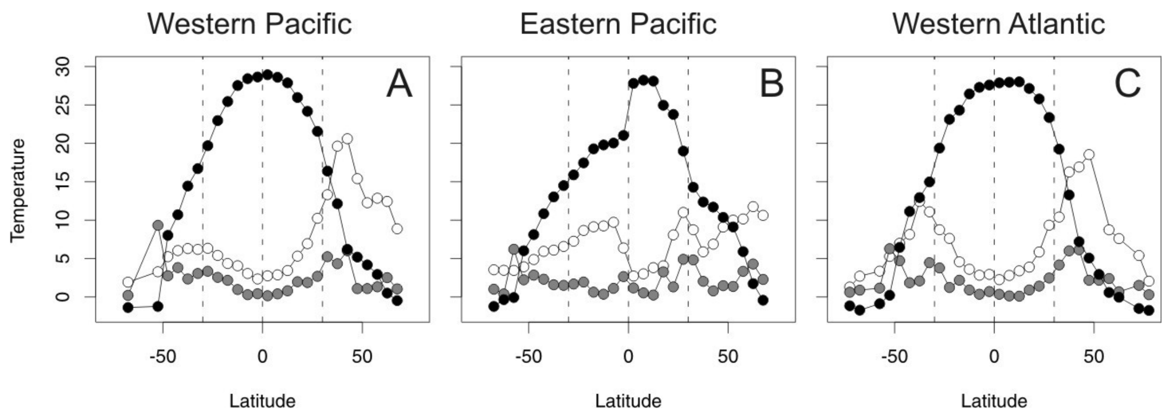

Figure A1 Annual mean daily sea-surface temperature (black circles) exhibits very low spatial variation at low latitudes and a steep decline in at mid latitudes in the Western Pacific and Western Atlantic. Absolute change in annual mean daily sea-surface temperature between 5° latitudinal bands (gray circles, measured from equator to poles) and total annual temperature range (i.e., difference between monthly minimum and maximum daily sea-surface temperatures, open circles) increase simultaneously from low to mid latitudes and then decrease towards poles in the Western Pacific and Western Atlantic. Sea-surface temperatures were scaled up to 5° latitudinal bands to accommodate variation in spatial resolution in the biotic data.

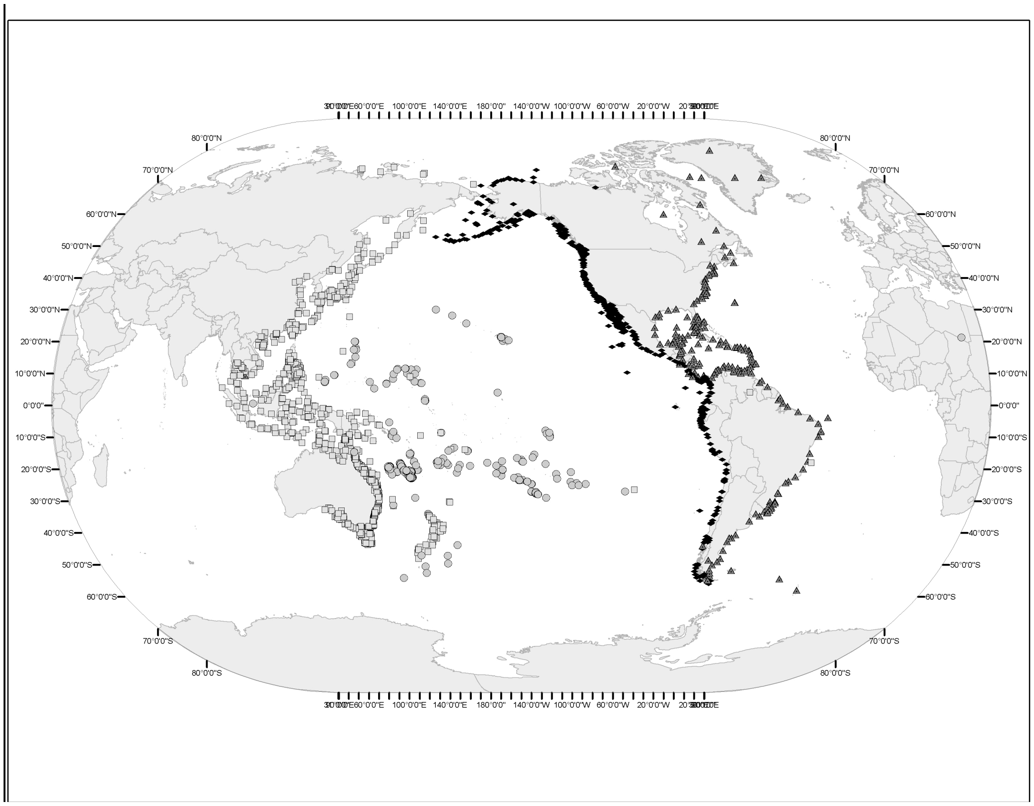

Figure A2 Localities with occurrence data used in the analyses of latitudinal and thermal ranges of individual species in this study. They are derived from the three best-sampled latitudinal "transects" -- the Western Pacific (gray squares), Eastern Pacific (black diamonds), and Western Atlantic (gray triangles). See Supplement text A for details.

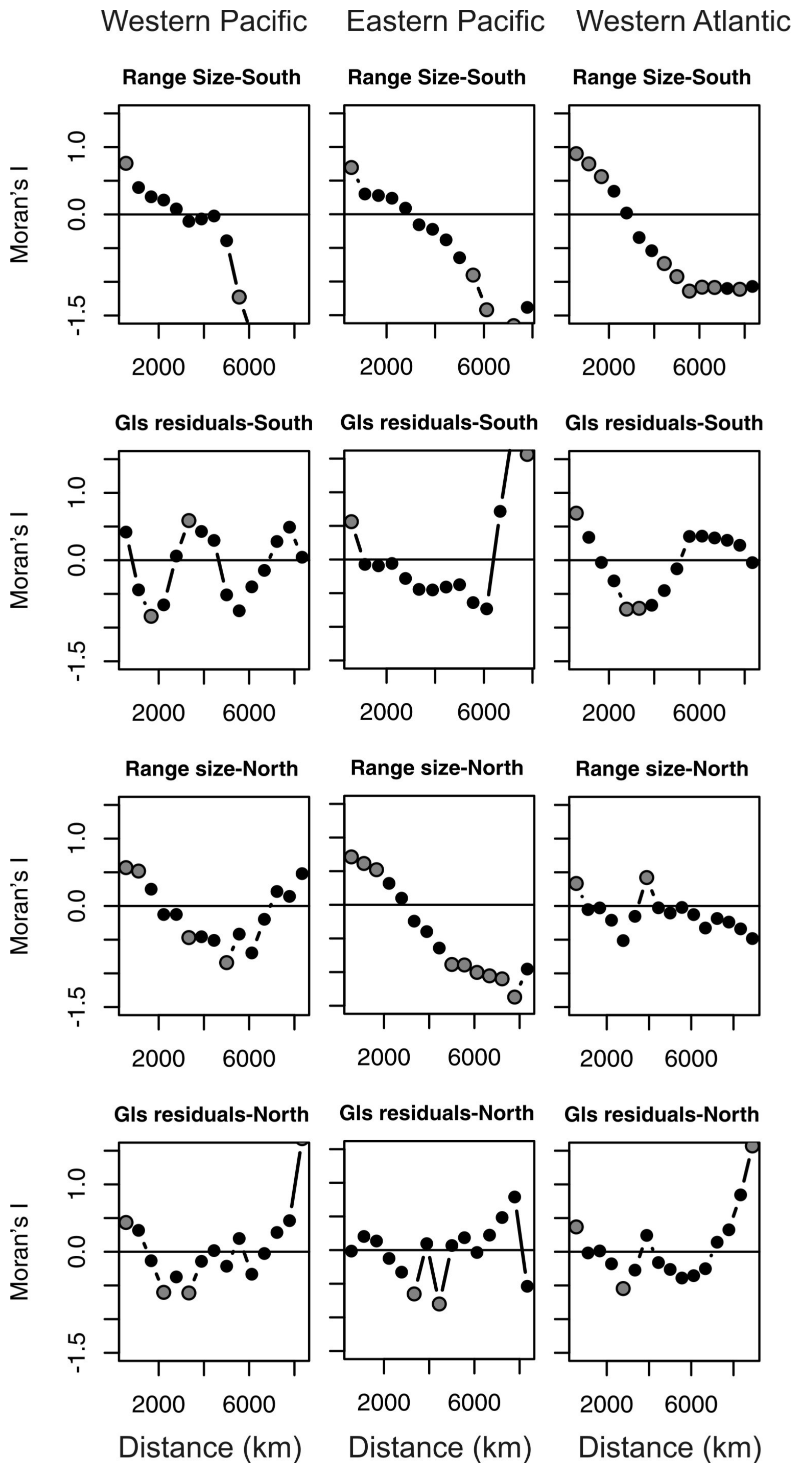

Figure A3 Spatial autocorrelation of range sizes and of the residuals from generalized-least square models in correlograms, using distance classes separated by 500 km (separately for the Northern and Southern Hemispheres). Gray points correspond to significant Moran's I coefficients at α=0.05.

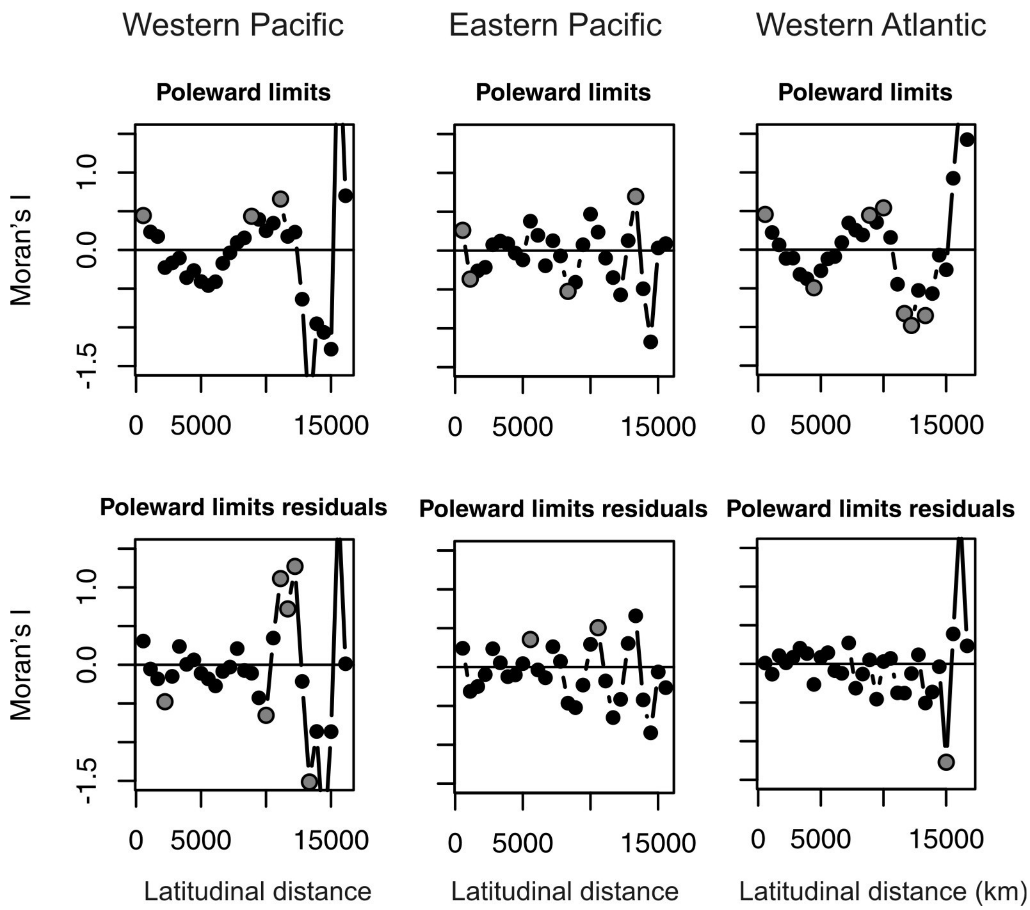

Figure A4 Spatial autocorrelation of the clustering of poleward range limits and of the residuals from generalized-least square models in correlograms, using distance classes separated by 500 km (separately for the Northern and Southern Hemispheres). Gray points correspond to significant Moran's I coefficients at α=0.05.

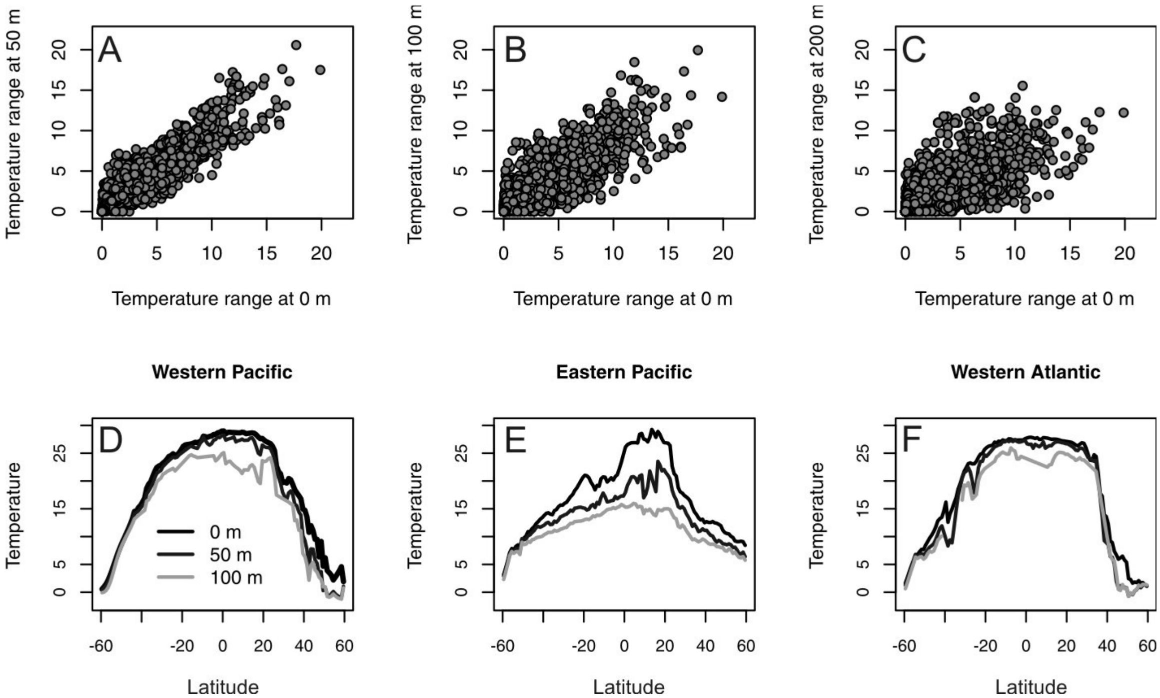

Figure A5 A-C. Relationships between temperature range encompassed by the geographic range of each species, calculated at the sea-surface and (A) 50 m, (B) 100 m and (C) 200 m indicate that species thermal ranges at 50 and 100 m remain highly significantly correlated with sea-surface temperature. The correlation between thermal range at 200 m with sea-surface temperature becomes weaker but remains highly significant. In a linear regression, the thermal range at 0 m explains 86% of variation in the range at 50 m (Pearson $r = 0.93$, $p < 0.0001$), 71% variation in the range at 100 m (Pearson $r = 0.84$, $p < 0.0001$), and 50% of variation in the thermal range at 200 m (Pearson $r = 0.71$, $p < 0.0001$). D-F. Latitudinal gradients in annual mean temperature have similar shapes at 0, 50, and 100 m along the three transects and remain flat at low latitudes at 100 m in the Western Pacific and Western Atlantic. Temperatures at 0 m, 50 and 100 m were obtained from the World Ocean Atlas 2005 at 1° latitude/longitude resolution.

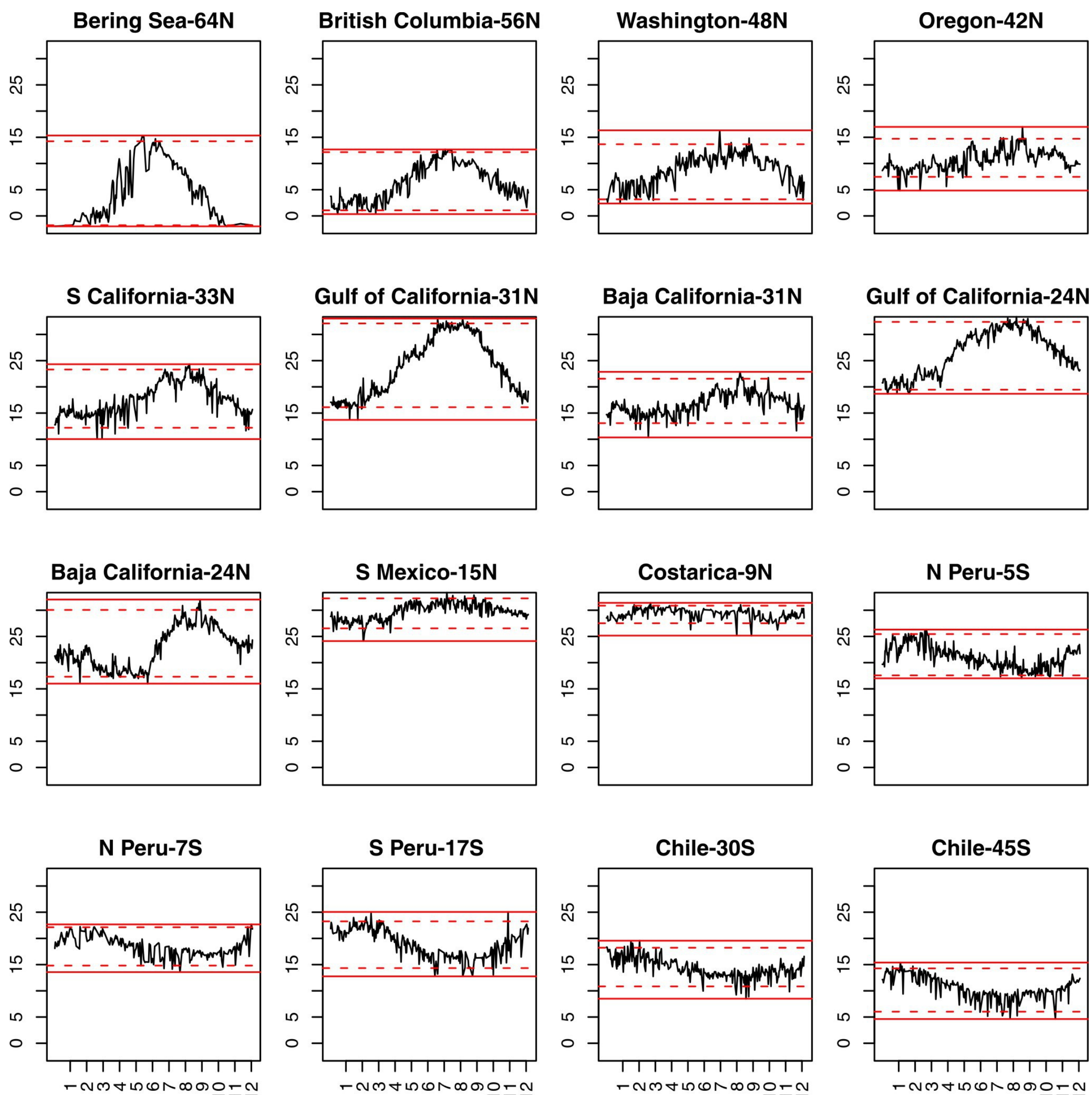

Figure A6 Annual SST daily minima and maxima based on the MODIS data for 12 months in 2009 (daily temporal resolution and 9-km spatial resolution) in the Eastern Pacific. Solid lines represent minima and maxima of all daily measurements. Dashed lines represent 5th and 95th quantiles that are less affected by outliers and reliably capture the range of daily temperatures measured over one year.

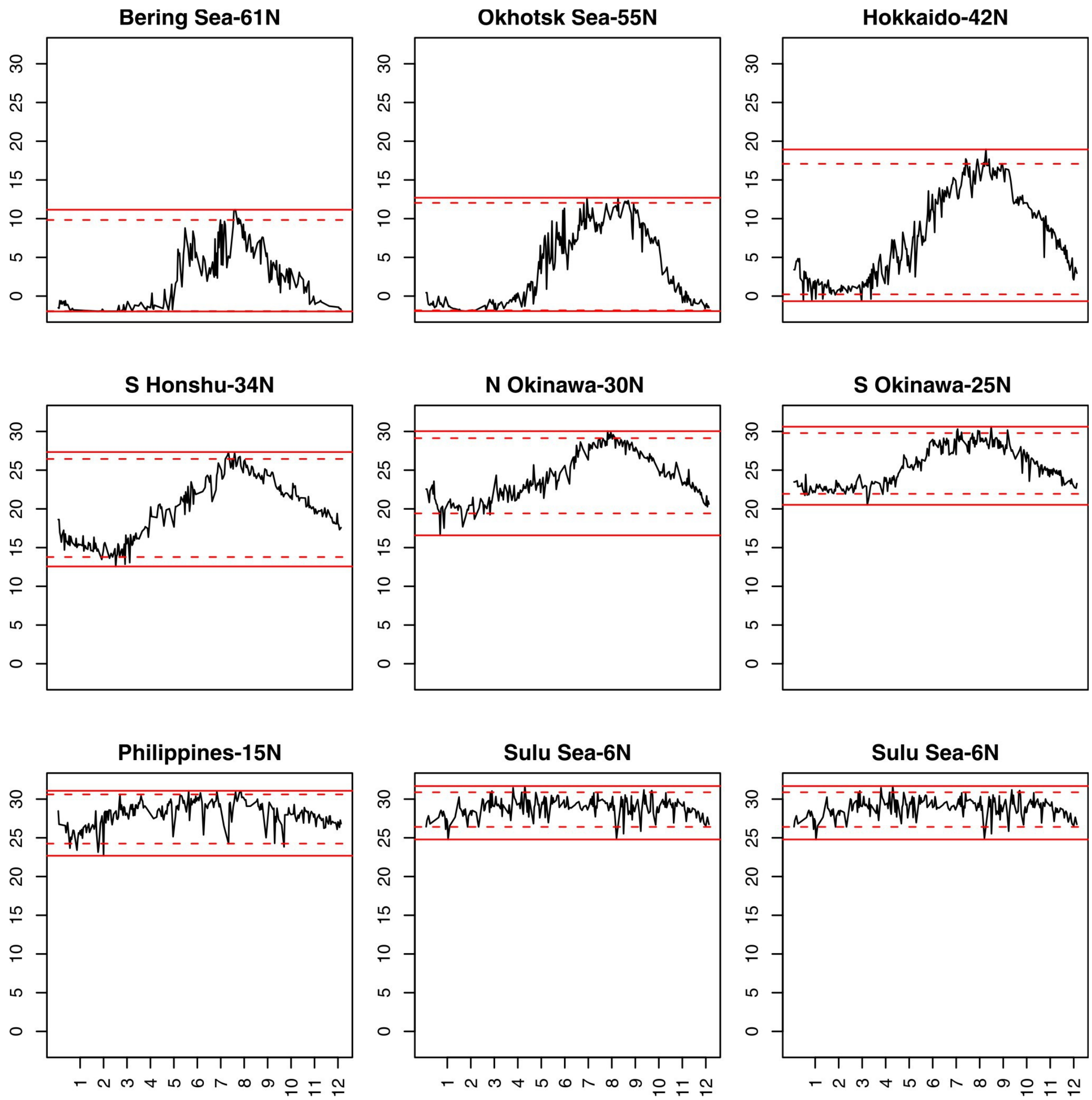

Figure A7 Examples of annual SST daily minima and maxima based on the MODIS data for 12 months in 2009 in the northern parts of the Western Pacific. Solid lines represent minima and maxima of all daily measurements. Solid lines represent minima and maxima of all daily measurements. Dashed lines represent 5th and 95th quantiles.

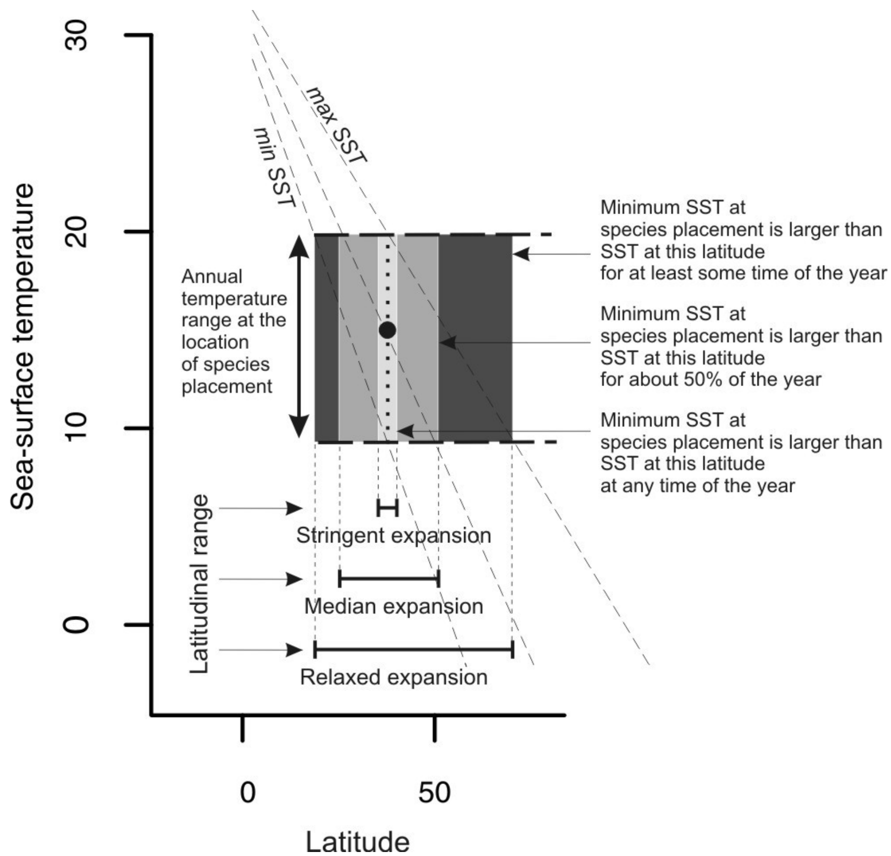

Figure A8 Three scenarios for latitudinal range expansion limited by annual daily SST minima and maxima. In the stringent scenario (light-grey range), species only occupy habitats that lie completely within the minimum and maximum temperature at their initial latitudinal location of placement (latitude of black point); in the median scenario (medium-gray range), species occupy habitats where SST falls between the minimum and maximum temperatures at the latitude of their placement for approximately 50% of the year, and in the relaxed scenario (dark-gray range) they can track habitats if SST remains within those bounds for at least some part of the year.

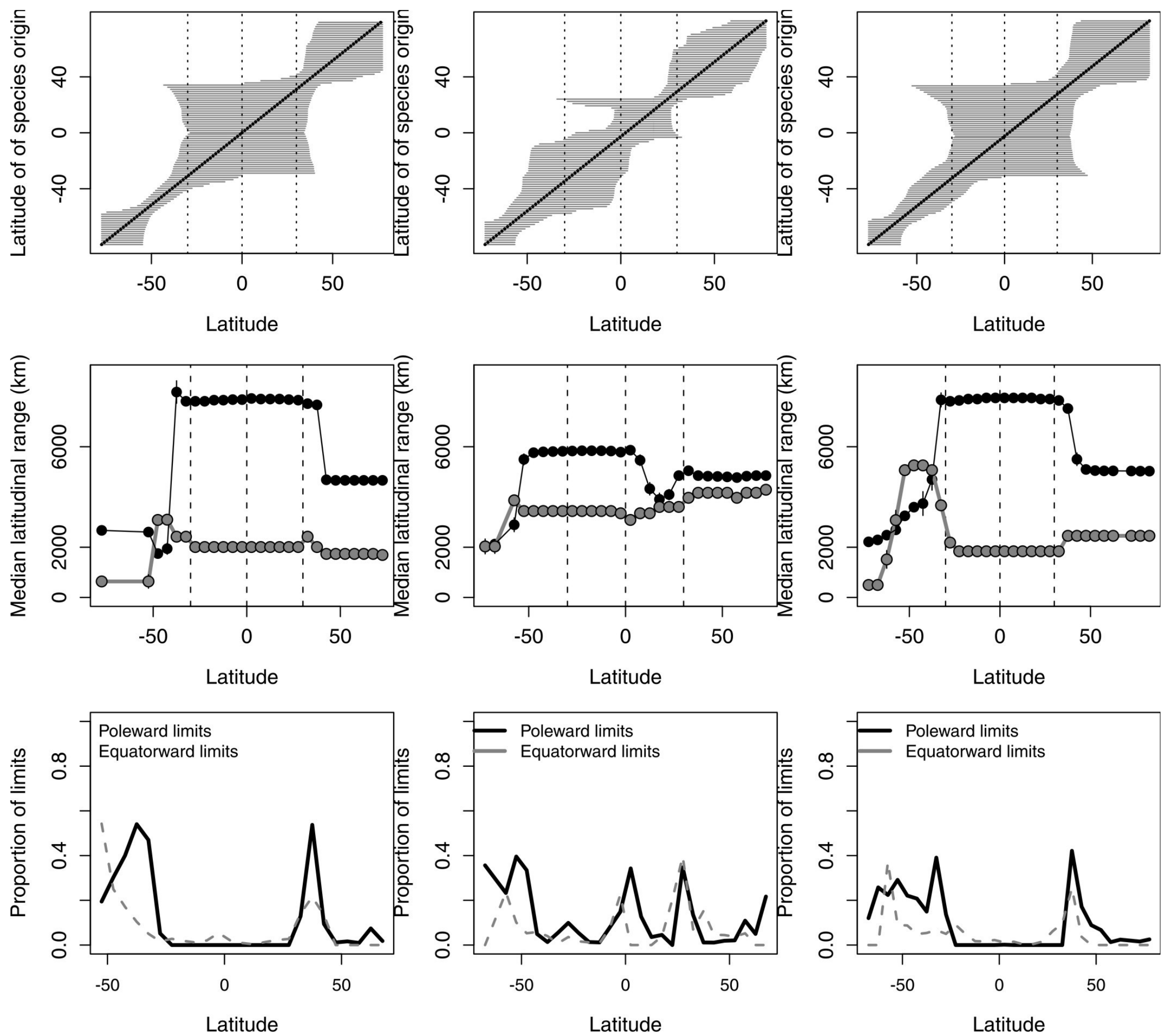

Figure A9 The relaxed temperature-limited model predicts patterns qualitatively similar to the median temperature-limited model. Latitudinal ranges (black circles) are largest at low latitudes (but also attain large sizes at 40-50° N and S) whereas thermal ranges (gray circles) are generally larger at high latitudes. The clustering of range limits shows a broad minimum at low latitudes and marked clustering at mid latitudes.

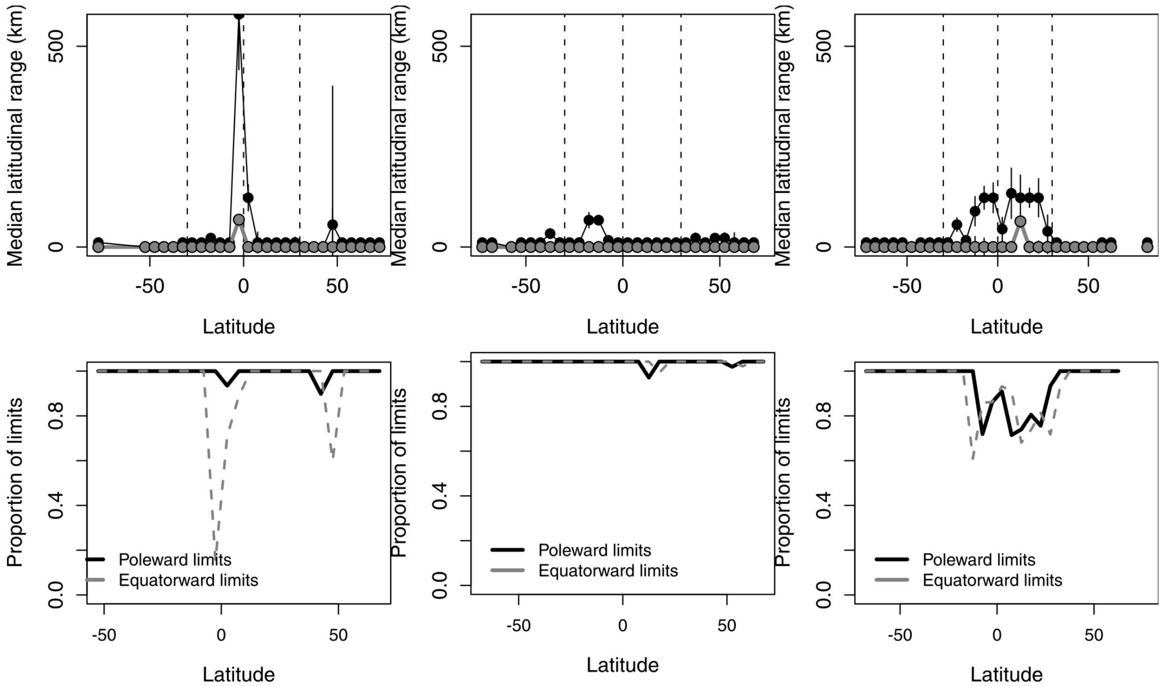

Figure A10 Range expansion is highly constrained in the stringent temperature-limited model. Latitudinal ranges will be largest at low latitudes (black circles in the top panel). The clustering of range limits is very high owing to small latitudinal range sizes along the whole gradient, but some minima do occur in a narrow region at low latitudes.

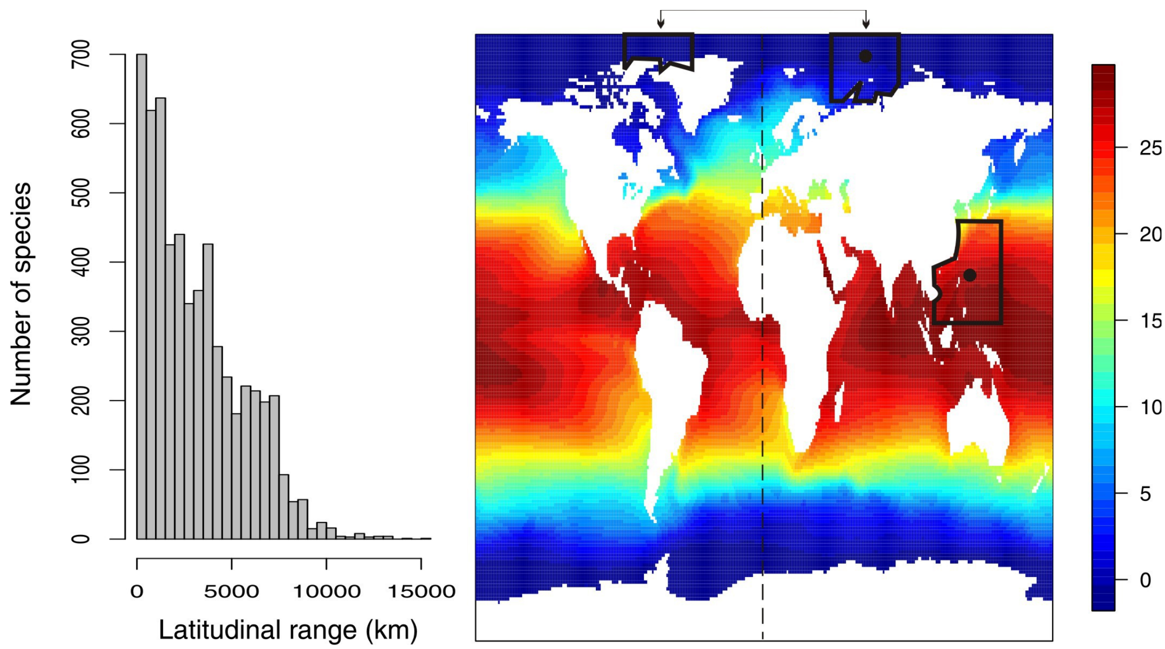

Figure A11 – Visualization of the range-shuffling null model in the equirectangular projection with mean annual SST values. In this example, two species with a latitudinal range of 30° or ~3,300 km are randomly placed on the sea. The probability of range midpoint-placement at a given latitude (black points) is weighted by the longitudinal extent (in km) of the corresponding 5° latitudinal band. After this placement, the latitudinal range is drawn from the empirical size-frequency distribution of latitudinal ranges on the left (each empirical latitudinal range has a corresponding longitudinal range that sets the longitudinal dimension of the rectangle). If the entire southern or northern edge of the range falls on a continent, that range is rejected and midpoint placement is repeated. If the range falls outside the grid edge, it is transported into the adjacent hemisphere to avoid range truncation (see the example of the range placed close to the North Pole).

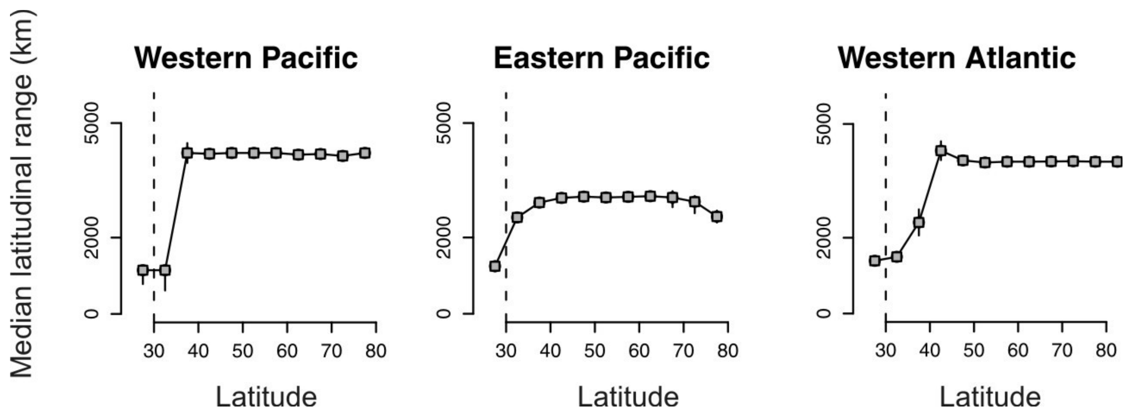

Figure A12 - Modeled gradients in median latitudinal range size per 5° latitudinal band, measured as the median of all ranges that occur in that band, in domains with southern boundary at 25°N: temperature-limited models predict that median latitudinal ranges will increase with latitudes.

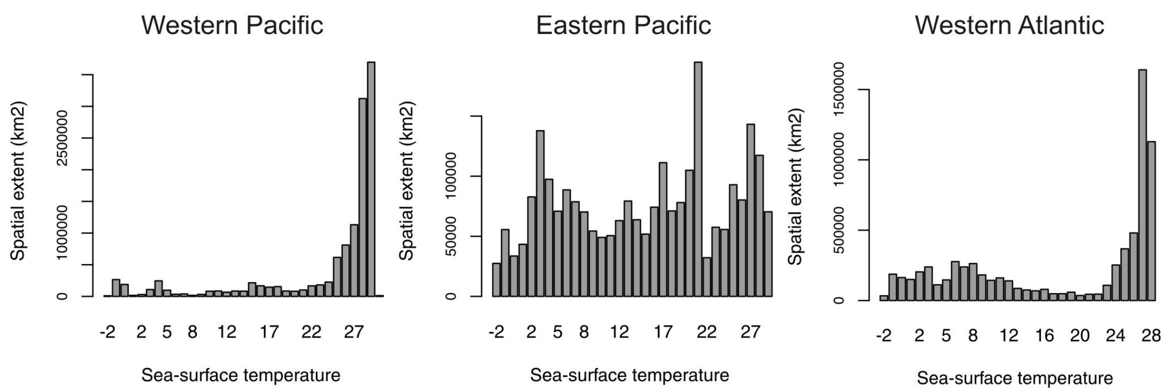

Figure A13 The spatial extent (areal coverage in km^2) of sea-surface temperature for (A) 1° shelf cells in the Western Pacific, Eastern Pacific, and Western Atlantic. Warm sea-surface temperatures dominate the frequency distribution of temperature classes and form a continuous band on both sides of the equator at low latitudes along the western ocean margins.

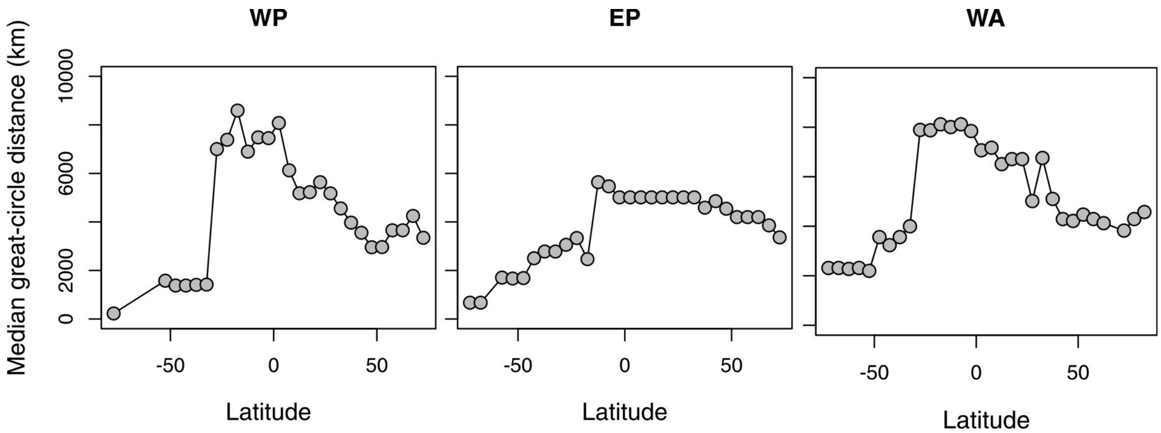

Figure A14 Empirical median great-circle distance range size is largest at low latitude, similarly as median latitudinal range size.